

Research on advancing chromatic reproduction and luminosity of a WLED using triple-layer remote phosphor arrangement

Ha Thanh Tung¹, Huu Phuc Dang²

¹Faculty of Basic Sciences, Vinh Long University of Technology Education, Vietnam

²Faculty of Fundamental Science, Industrial University of Ho Chi Minh City, Ho Chi Minh City, Vietnam

Article Info

Article history:

Received Sep 27, 2021

Revised Jul 30, 2022

Accepted Dec 26, 2022

Keywords:

CaLaB3O7:Ce³⁺,Mn²⁺

Color quality

MgB2O4:Mn²⁺

Triple-layer structure

WLEDs

ABSTRACT

In this study, the use of triple-sheet phosphor arrangement (TRP) in performing significant improvements to both color quality and luminous flux of white light emitting diode (WLEDs) is introduced. The phosphor layer of CaLaB3O7:Ce³⁺,Mn²⁺ is to accomplish green-spectra enhancement for the boost of luminous efficacy (LE), while MgB2O4:Mn²⁺ red phosphor layer is for red-spectra enhancement to better color rendering index (CRI) of WLEDs. The changes in these two phosphors' concentrations present considerable effects on the yellow phosphor YAG:Ce³⁺ concentration, the color quality scale (CQS), CRI, and LE. Findings display the decrease of YAG:Ce³⁺ concentration accompanying the increase of red and green phosphor concentrations, for the stabilized average correlated color temperatures (ACCTs) between 6000 and 8500 K. Results also reveal that greater content of MgB2O4:Mn²⁺ leads to greater CRI value. Meanwhile using the increasing CaLaB3O7:Ce³⁺,Mn²⁺ concentration, the CRI lowers considerably. CQS, on the other hand, can increase with CaLaB3O7:Ce³⁺,Mn²⁺ concentration from 10% to 14%. Especially, given the enhancement for the CRI as well as CQS, LE value will surge to more than 40% due to the reduction of scattering light and the addition of green light. The outcome of the study is a priceless reference for light emitting diode (LED) producers.

This is an open access article under the [CC BY-SA](https://creativecommons.org/licenses/by-sa/4.0/) license.



Corresponding Author:

Huu Phuc Dang

Faculty of Fundamental Science, Industrial University of Ho Chi Minh City

Ho Chi Minh City, Vietnam

Email: danghuuphuc@iuh.edu.vn

1. INTRODUCTION

The age of solid-state illumination system is introduced by the white light-emitting diodes (WLEDs) which are of significant luminous efficiency (LE), extended in the period of efficacy, low in energy usage, and eco-friendly to the environment. WLEDs are commonly applied in lighting systems such as auto lamps and displays [1], [2]. The recent regular WLED formation has been the compound containing a blue-excited LED along with a YAG:Ce³⁺ sheet [3]. A part of blue light emission is produced by the Stokes change, resulting in the longer-wavelength yellow light. This is followed by a merger between blue as well as yellow illumination that creates white emissions. The compound of phosphorus powders and organic silicone or other organic chemical components is the most popular phosphor layer compound [4], [5]. Still, extreme stimulation or intense environments are likely to cause degradation and deformation of the film. To perform good maintenance for the chemical and physical condition of the high-power WLED, the phosphor structuring model was equipped with phosphor-glass and phosphor-ceramic composites. The phosphor-glass composite applied in the phosphor-in-glass (PiG) structure is the combination of phosphor powders and glass matrices [6].

The phosphor glass, however, expects the least complicated combination method and has a greater ability to change emission properties than the phosphor ceramics. Despite most recent updated packaging configurations of WLEDs, the remote phosphor (RP) packaging configuration derived from the PiG is the most viable structure for strong-performance WLEDs. The phosphor layer, however, is projected to experience a massive temperature rise due to the power loss defined by Stokes shift and light absorption under strong stimulation [7], [8]. The glass substrate's low thermal conductivity (TC) results in less effective heat dispersion from the phosphor film to radiators [9]. Thus, the changes in the thermal quenching, the color coordinate, the wavelength, the lighting inconsistency, and the lifespan decrease will cause a reduction in the light emission by more than one level in the magnitude due to the rising heat within the phosphor film of the package. Materials exhibiting high TC are applied to encourage the dispersion of generated phosphor-layer heat of PiG in WLEDs, as a result [10], [11]. The supported graphene material that has high TC (~600 W/m·K) was applied to the covering of PiG to optimize the thermal management in WLEDs.

Nevertheless, the use of high TC graphene is limited due to its difficult preparation and low transmission. The heat dispersion of optoelectronic devices is enhanced by the large bandgap material hexagonal boron nitride (hBN) with the TC reaching 600 W/m·K, yet some difficulties occur in the preparation of the high-quality materials [12], [13]. A sapphire substrate with a great TC of about 30 W/m·K and high transmitting efficiency of up to ninety percent [14] was introduced as an alternative to the conventional low-TC glass substrate (<1.5 W/m·K) for the PiG to increase the thermal dispersion in phosphor layers. The higher the power conditions, the more enhancement would be seen. This study proposes a triple-film remote phosphor arrangement (TRP) for WLED models having a chromatic correlated temperature (CCT) of 6000 K [15]. Three phosphor sheets applied in this RP type are YAG:Ce³⁺, CaLaB₃O₇:Ce³⁺,Mn²⁺, and MgB₂O₄:Mn²⁺. The CaLaB₃O₇:Ce³⁺,Mn²⁺ with green emission is responsible for boosting the green-spectrum power for the aim of stronger luminous flux [16], [17]. Meanwhile, MgB₂O₄:Mn²⁺ will function as a booster for red-light energy to enhance the chroma reproduction quality. The collected data and presented figures show the outstanding enhancement in both color reproduction and the luminosity of the 8500-K WLED as long as the balance among primary blue, green, yellow, and red colors is kept.

2. PREPARATION

2.1. Preparation of phosphor materials

Compositions of red-phosphor MgB₂O₄:Mn²⁺ and green-phosphor CaLaB₃O₇:Ce³⁺,Mn²⁺ are integral aspects for our research. To obtain high-performance phosphor powders for the most accurate simulated and analyzed data, strict and careful phosphor preparation is required [18]. The composition details of both red-phosphor and green-phosphor, MgB₂O₄:Mn²⁺ and CaLaB₃O₇:Ce³⁺,Mn²⁺, are presented in Table 1 and Table 2, respectively. To get a well-prepared red-emission phosphor powder MgB₂O₄:Mn²⁺, the chemical mixture formed by dry-milled MgO, MnCO₃, and H₃BO₃ must be heated up in an open quartz boat three times. After every firing time, the mixture will be ground into powder. The first time, the operating temperature is 500 °C, and the flux of N₂ is added during the procedure. The second time also last 1 hour with the addition of N₂ flux but at 700 °C. The final firing time is operated at 1000 °C for 2 hours or 850 °C for 4 hours with N₂ flux. After the third heating stage finishes, the desired red-phosphor MgB₂O₄:Mn²⁺ is obtained with the emission energy peaking at 1.88 eV and 2.11 eV.

Table 1. Red-phosphor MgB₂O₄:Mn²⁺ composition details

Chemical elements	Mole percentage	By weight (g)
MgO	98	40
MnCO ₃	2	2.3
H ₃ BO ₃	205	127

Table 2. Green-phosphor CaLaB₃O₇:Ce³⁺,Mn²⁺ composition details

Chemical elements	Mole percentage	By weight (g)
CaCO ₃	95	95
La ₂ O ₃	98 (of La)	160
MnCO ₃	5	5.8
CeO ₂	2	3.4
H ₃ BO ₃	310	192

For the green-phosphor CaLaB₃O₇:Ce³⁺,Mn²⁺ preparing process, the initial step is to well-blended all the ingredients by dry grinding. Then, a series of three burning operations is carried out in open quartz boats, each of which will be followed by a powdering step. The first operation is at 500 °C with air flow.

The next firing time is performed with N_2 flow at $700\text{ }^\circ\text{C}$ for 1 hour while the operating temperature and time, as well as the added flow of the third firing, are $900\text{ }^\circ\text{C}$, 2 hours, and CO, respectively. The final phosphor product will exhibit a discharge in green hue yielding an apex emission energy measured at 2.40 eV [19].

2.2. Simulation of TRP

To perform the TRP arrangements with the RP-WLED of 8500 K CCT, the commercial software LightTools 9.0 equipped with the Monte Carlo technique was utilized. The optical 3-D physical simulation and a real sample of RP-WLED are illustrated in Figure 1. The reflector in this type possesses bottom length measured at 8 mm, a height measured at 2.07 mm, as well as length measured at 9.85 mm at its top surface, see Figure 1(a). WLEDs have a 0.08 mm thick remote phosphor coating that sits on top of nine LED chips, as shown in Figure 1(b). In a bottom-to-top order, the TRP structure is made up of three separate phosphor layers of yellow-emitting $YAG:Ce^{3+}$, green-emitting $CaLaB_3O_7:Ce^{3+},Mn^{2+}$, and red-emitting $MgB_2O_4:Mn^{2+}$, see Figure 1(c). Each square chip is 1.14 mm long with a 0.15 mm height, affixed to the reflector's chamber. Each blue chip with a wavelength of 455 nm emits 1.16 W of radiant flux, as displayed in Figure 1(d). The contents for granules of phosphor fluctuates continually from 2 to 20 percent to investigate its impacts on the TRP-WLED properties [20].

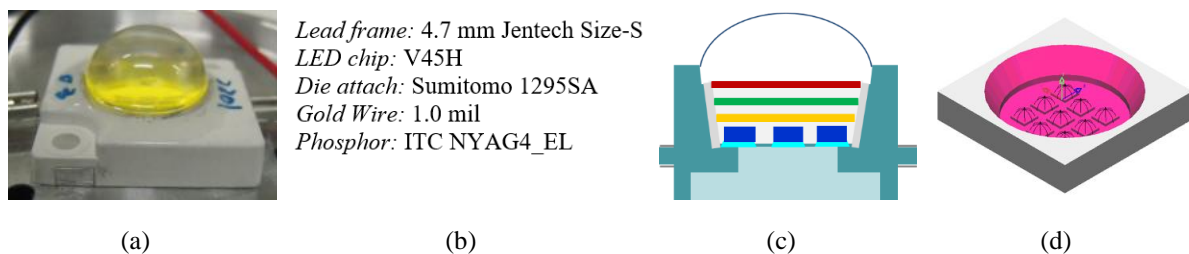


Figure 1. The schematic illustrations of (a) a real PiG-WLED sample, (b) its parameters, (c) a TRP arrangement, and (d) the 3D physical simulation of a WLED

3. RESULTS AND DISCUSSION

The study firstly assesses the color reproduction quality corresponding to the varying concentration of red and green phosphors, $MgB_2O_4:Mn^{2+}$ and $CaLaB_3O_7:Ce^{3+},Mn^{2+}$. The essential parameters for this assessment are the color rendering intent (CRI) along with color quality scale (CQS), which are illustrated in Figure 2 and Figure 3, respectively. In Figure 2, when the red phosphor weight percentage (wt%) is increased within the range of 2–20wt%, the CRI value progressively rises until it reaches the highest points at 20 wt% of $MgB_2O_4:Mn^{2+}$. The increasing green-phosphor concentration, on the other hand, is detrimental to the CRI. The evidence is the significant decline of the CRI data at higher concentrations of green phosphor, irrespective of the increase in red-phosphor concentration. At the same 20 wt%, for instance, the red phosphor shows the greatest CRI while the green phosphor reduced the CRI to the lowest level, inferred from Figure 2. These results have confirmed that increasing the red spectra in the visible wavelength of generated white light with $MgB_2O_4:Mn^{2+}$ phosphor is required to raise CRI values [21]. Since the red spectral energy improvement is known as a benefit to CRI, the green spectra enhancement is considered a drawback that degrades the color rendition. Moreover, as the green-phosphor $CaLaB_3O_7:Ce^{3+},Mn^{2+}$ is used at higher concentration, this means a larger proportion of green light is produced and may become redundant, which is probably not conducive to CRI. Additionally, regarding the organizational arrangement of the TRP, the phosphor sheet of green-emitting $CaLaB_3O_7:Ce^{3+},Mn^{2+}$ is located beneath the red-emitting $MgB_2O_4:Mn^{2+}$ sheet, allowing both blue and yellow light to interact with the green phosphor particles before reaching red ones. Consequently, the conversion power of the $MgB_2O_4:Mn^{2+}$ sheet decrease as the layer of phosphor on green concentration increases. As such, the green phosphor $CaLaB_3O_7:Ce^{3+},Mn^{2+}$ concentration should be at its minimum to reach the goal of high CRI.

As mentioned, the color reproduction efficiency of the TRP will be validated through either the CRI or CQS. The CRI has been recognized to have flaws in presenting the real color of the targeted objects. Under the light of the high intensity of blue or red emission color, the CRI provided high rendering scores. Therefore, the CRI is just a single aspect of color reproduction efficiency. There are other two factors that are crucial to validate the chromatic reproduction effect of a WLED, including the coordination of color elements on the chroma scale and the visual inclination of users. The CQS has been introduced to cover all these three critical factors, becoming a nearly perfect measurement for the color reproduction effect in illumination. Consequently, when taking these two accessing color parameters into consideration, CQS probably presents a more sufficient assessment than CRI, and thus, becomes more challenging to manage for high values [22]-[24].

The question is how can we increase the CQS of a WLED? is it possible to just simply increase only red spectra for CQS enhancement as the CRI? Figure 3 shows the CQS values as well as the answers to the previous questions. Generally, CQS is also increased as the red phosphor concentration $MgB_2O_4:Mn^{2+}$ rose. However, unlike the variation in CRI, the variation in CQS is small when the green phosphor layer $CaLaB_3O_7:Ce^{3+},Mn^{2+}$ concentration is adjusted. The CQS data in Figure 3 can confirm that phosphors in red as well as green help increase the CQS. Greater CQS requires achieving a color balance of critical colors, including green, yellow, red, and blue. As the concentration for said phosphors rises, the content of $YAG:Ce^{3+}$ declines, sustaining the CCT at 8500 K.

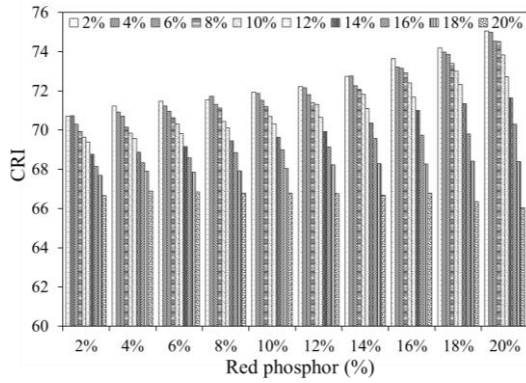


Figure 2. CRI value in TRP with various concentrations for $MgB_2O_4:Mn^{2+}$ and green $CaLaB_3O_7:Ce^{3+},Mn^{2+}$ at 8500 K

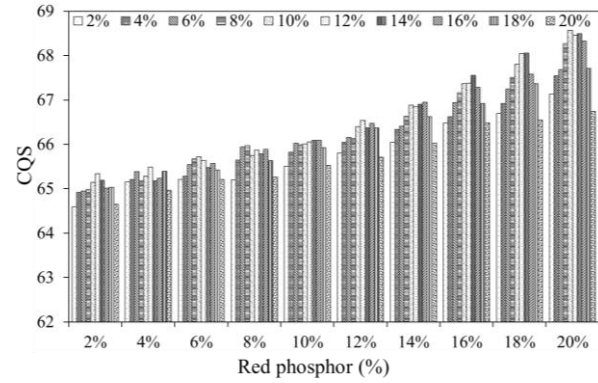


Figure 3. CQS value in TRP with various concentrations for $MgB_2O_4:Mn^{2+}$ as well as $CaLaB_3O_7:Ce^{3+},Mn^{2+}$ at 8500 K

Decreasing $YAG:Ce^{3+}$ content leads to less yellow spectral content, which has two benefits. The first would be limiting illumination scattering backward to the chip in LED surface which usually leads to reabsorption, resulting in a large proportion of extracted light, allowing an increase in luminous flux to be presented. Another advantage is that yellow-light components which replace the blue light element, as well as the red and green light elements are reduced. The control of CQS is the control over these 3 light color elements. CQS improves steadily when the $CaLaB_3O_7:Ce^{3+},Mn^{2+}$ content increases (2% – 10%) and gradually declined afterwards. The biggest values of CQS are recognized with 10% to 14% in the concentration of $CaLaB_3O_7:Ce^{3+},Mn^{2+}$. The yellow illumination factor is dominant even with a modest green-phosphor concentration (2% – 10%). The light-transmitting energy losses are initiated by the scattering in a backward direction and eventually prevent the CQS from acquiring the best value. If we increase the green-emitting $CaLaB_3O_7:Ce^{3+},Mn^{2+}$ concentration to the range of 10% – 14%, the green-spectra portion will be sufficient for higher CQS and could achieve the maximum.

However, when the concentration of $CaLaB_3O_7:Ce^{3+},Mn^{2+}$ increases, the green light portion is exorbitant, breaking the balance among the mentioned essential color elements. As a result, the higher the concentration of green phosphor, the more CQS values decrease. Remote phosphor structures have more comprehensive hue output control, surpassing conformal as well as in-cup phosphor systems. Such control will be more strenuous for RP-WLEDs with the CCT greater than 8500 K (such as 7000 K – 8500 K). Additionally, to reduce the number of backscatter events, the TRP helps to increase the internal scattering activities of the WLED. The mixing of light components increases as dispersion increases, culminating in desirable white illumination. Is such an increased dispersion, however, causing the energy to transmit less light? The simulation of calculation for the conveyed blue illumination as well as transformed yellow illumination within the dual-sheet configuration, causing significant enhancement in LED efficiency, will be illustrated, and explained in this part. In a single-layer RP, the phosphor layer has a $2h$ thickness, and the computation of both conveyed blue illumination as well as transformed yellow illumination is stated as the [25].

$$PB_1 = PB_0 \times e^{-2\alpha_{B1}h} \tag{1}$$

$$PY_1 = \frac{1}{2} \frac{\beta_1 \times PB_0}{\alpha_{B1} - \alpha_{Y1}} (e^{-2\alpha_{Y1}h} - e^{-2\alpha_{B1}h}) \tag{2}$$

In the dual-film RP, the phosphor sheet's breadth will be h , and subsequently, the conveyed blue illumination as well as transformed yellow illumination will be possibly performed.

$$PB_2 = PB_0 \times e^{-2\alpha_{B2}h} \quad (3)$$

$$PY_2 = \frac{1}{2} \frac{\beta_2 \times PB_0}{\alpha_{B2} - \alpha_{Y2}} (e^{-2\alpha_{Y2}h} - e^{-2\alpha_{B2}h}) \quad (4)$$

The h represents a phosphor sheet's thickness. Subscript numbers 1 and 2 are used to mark the single- and dual-film RPs. The transmutation fraction for transforming the blue illumination into yellow illumination would be β . The yellow-light reflection coefficient is shown by γ . The light power generated by the blue LED comprises the blue illumination (PB) along with the yellow illumination (PY), which is indicated via PB_0 . The ratios concerning the waste of power for the blue as well as yellow illumination during their generation within the layer of phosphor are accordingly αB , αY .

In comparison, the efficiency of illumination from WLEDs of the dual-film RP has greater performance, surpassing the one-film configuration:

$$\frac{(PB_2 + PY_2) - (PB_1 + PY_1)}{PB_1 + PY_1} > 0 \quad (5)$$

The analysis of the dispersion for the spherical granules of phosphor is supported by the Mie hypothesis for dispersion. Besides, with the law of Lambert-Beer, the power for transmitted light could be computed [26]:

$$I = I_0 \exp(-\mu_{ext}L) \quad (6)$$

For the equation, the incident illumination energy will be presented by I_0 , and the thickness of the phosphor sheet is L in mm. The extinction coefficient is μ_{ext} which is demonstrated as $\mu_{ext} = N_r \times C_{ext}$. Correspondingly, N_r indicates the density-allocation number for phosphor granules (mm^{-3}). C_{ext} indicates the extinction cross-section for spherical granules.

Using extra phosphor layers increases the flux output of WLEDs' illumination, as shown in (5). The increase in concentrations of both red $\text{MgB}_2\text{O}_4:\text{Mn}^{2+}$ and green $\text{CaLaB}_3\text{O}_7:\text{Ce}^{3+}, \text{Mn}^{2+}$ increases the luminous flux at 8500 K, as depicted in Figure 4. When these two phosphor concentrations show a rise, lowering YAG: Ce^{3+} content would vital when it comes to the CCT's stability. As demonstrated, one of the advantages of having decreased yellow-phosphor concentration is the lower waste of illumination energy caused by backwardly redirected illumination scatterings. Furthermore, this decline leads to higher internal transmission energy, inferred from (6) based on Beer's law. As a result, the increase in either $\text{CaLaB}_3\text{O}_7:\text{Ce}^{3+}, \text{Mn}^{2+}$ concentration or $\text{MgB}_2\text{O}_4:\text{Mn}^{2+}$ concentration can yield more luminous flux. According to the results shown in Figure 4, $\text{CaLaB}_3\text{O}_7:\text{Ce}^{3+}, \text{Mn}^{2+}$ increasing weight percentages help the luminous efficiency (LE) increase by more than 40%, without regard to $\text{MgB}_2\text{O}_4:\text{Mn}^{2+}$ concentrations. The result obtained is a useful guide for the manufacturer in determining the proper concentration of the two phosphors. For example, with an aim at good CQS accompanying high-value LE, the concentration percentages of $\text{CaLaB}_3\text{O}_7:\text{Ce}^{3+}, \text{Mn}^{2+}$ must be between 10 and 14wt%, while the concentration percentage of $\text{MgB}_2\text{O}_4:\text{Mn}^{2+}$ stays at 20 wt%.

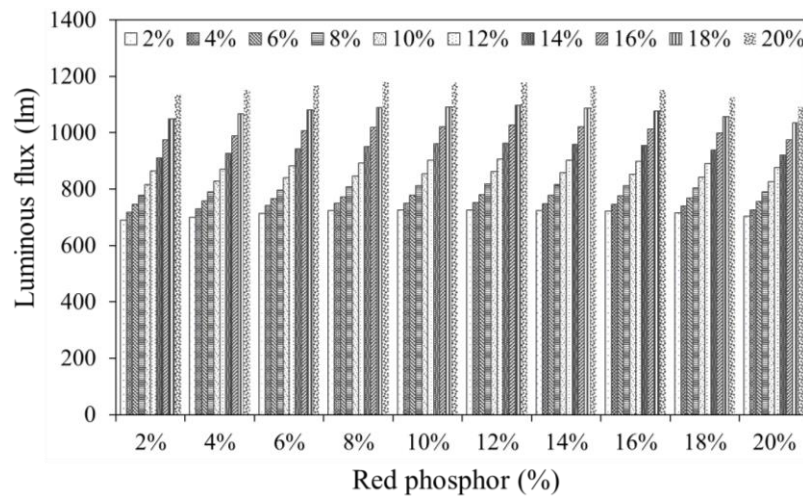


Figure 4. Lumen in TRP with various concentrations for $\text{MgB}_2\text{O}_4:\text{Mn}^{2+}$ as well as $\text{CaLaB}_3\text{O}_7:\text{Ce}^{3+}, \text{Mn}^{2+}$ at 8500 K

4. CONCLUSION

The use of a TRP arrangement with two phosphors of green $\text{CaLaB}_3\text{O}_7:\text{Ce}^{3+},\text{Mn}^{2+}$ and red $\text{MgB}_2\text{O}_4:\text{Mn}^{2+}$ for the improvement in CRI, CQS, and LE of WLEDs' illumination at 8500 K has been proposed. Not only is the color quality improved with the TRP construction, but also the LE, which is seldom demonstrated in previous configurations. Balancing yellow, green, and red chroma of the white light must be focused and preserved in processing TRP structure for higher efficiency. This can be operated by adjusting the concentrations of $\text{CaLaB}_3\text{O}_7:\text{Ce}^{3+},\text{Mn}^{2+}$ and $\text{MgB}_2\text{O}_4:\text{Mn}^{2+}$. The green light component of WLEDs is controlled by the green layer $\text{CaLaB}_3\text{O}_7:\text{Ce}^{3+},\text{Mn}^{2+}$ phosphor, allowing the increase in luminosity of the RP-WLED. The additional phosphor layer in TRP, moreover, helps heighten the luminous intensity, much more than that of the single-layer RP. Additionally, controlling red layer $\text{MgB}_2\text{O}_4:\text{Mn}^{2+}$ concentration allows the control over red spectral components within the visible wavelength of white illumination from a WLED, leading to an increase in CRI. The study also demonstrates that lowering concentrations of yellow-phosphor $\text{YAG}:\text{Ce}^{3+}$ helps balance yellow, green, red, and blue color distribution on the chroma scale while initiating a reduction in the backward-directed scattering, which contributes to enabling the best color reproduction effects and the highest luminosity.




REFERENCES

- [1] Y. Shi, S. Ye, J. Yu, H. Liao, J. Liu, and D. Wang, "Simultaneous energy transfer from molecular-like silver nanoclusters to $\text{Sm}^{3+}/\text{Ln}^{3+}$, $\text{Ln}=\text{Eu}$ or Tb . in glass under UV excitation," *Optics Express*, vol. 27, pp. 38159-38167, 2019, doi: 10.1364/OE.380860.
- [2] M. E. Kandel, W. Lu, J. Liang, O. Aydin, T. A. Saif, and G. Popescu, "Cell-to-cell influence on growth in large populations," *Biomedical Optics Express*, vol. 10, pp. 4664-4675, 2019, doi: 10.1364/BOE.10.004664.
- [3] H. Daicho, K. Enomoto, H. Sawa, S. Matsuishi, and H. Hosono, "Improved color uniformity in white light-emitting diodes using newly developed phosphors," *Optics Express*, vol. 26, no. 19, pp. 24784-24791, 2018, doi: 10.1364/OE.26.024784.
- [4] Y. Wu *et al.*, "Monolithic integration of MoS₂-based visible detectors and GaN-based UV detectors," *Photonics Research*, vol. 7, no. 10, pp. 1127-1133, 2019, doi: 10.1364/PRJ.7.001127.
- [5] B. Jain *et al.*, "High performance electron blocking layer-free InGaN/GaN nanowire white-light-emitting diodes," *Optics Express*, vol. 28, no. 1, pp. 665-675, 2020, doi: 10.1364/OE.28.000665.
- [6] C. Su, X. Liu, and J. Zhang, "Analysis of the errors of the integrating sphere for the transmittance of nonplanar optical components," *Journal of Optical Technology*, vol. 85, no. 1, pp. 42-47, 2018, doi: 10.1364/JOT.85.000042.
- [7] X. Bao *et al.*, "User-centric quality of experience optimized resource allocation algorithm in VLC network with multi-color LED," *Optics Express*, vol. 26, no. 21, pp. 27826-27841, 2018, doi: 10.1364/OE.26.027826.
- [8] J.-S. Li, Y. Tang, Z.-T. Li, L.-S. Rao, X.-R. Ding, and B.-H. Yu, "High efficiency solid-liquid hybrid-state quantum dot light-emitting diodes," *Photonics Research*, vol. 6, pp. 1107-1115, 2018, doi: 10.1364/PRJ.6.001107.
- [9] J. Chen *et al.*, "Fabrication of $\text{Tb,Gd}_3\text{Al}_5\text{O}_{12}:\text{Ce}^{3+}$ phosphor ceramics for warm white light-emitting diodes application," *Optical Materials Express*, vol. 9, no. 8, pp. 3333-3341, 2019, doi: 10.1364/OME.9.003333.
- [10] L. Xu, B. Zhao, and M. R. Luo, "Color gamut mapping between small and large color gamuts: part II. gamut extension," *Optics Express*, vol. 26, no. 13, pp. 17335-17349, 2018, doi: 10.1364/OE.26.017335.
- [11] H. L. Ke *et al.*, "Lumen degradation analysis of LED lamps based on the subsystem isolation method," *Applied Optics*, vol. 57, no. 4, pp. 849-854, 2018, doi: 10.1364/AO.57.000849.
- [12] J. Cheng *et al.*, "Luminescence and energy transfer properties of color-tunable $\text{Sr}_x\text{La}_{1-x}\text{PO}_4:\text{Ce}^{3+},\text{Tb}^{3+},\text{Mn}^{2+}$ phosphors for WLEDs," *Optical Materials Express*, vol. 8, no. 7, pp. 1850-1862, 2018, doi: 10.1364/OME.8.001850.
- [13] S. Feng and J. Wu, "Color lensless in-line holographic microscope with sunlight illumination for weakly-scattered amplitude objects," *OSA Continuum*, vol. 2, no. 1, pp. 9-16, 2019, doi: 10.1364/OSAC.2.000009.
- [14] C. Jaques, E. Pignat, S. Calinon, and M. Liebling, "Temporal super-resolution microscopy using a hue-encoded shutter," *Biomedical Optics Express*, vol. 10, no. 9, pp. 4727-4741, 2019, doi: 10.1364/BOE.10.004727.
- [15] Z. Liu *et al.*, "Effect of the replacement of Zn^{2+} with Mg^{2+} in $\text{Ca}_{14}\text{Zn}_6\text{Ga}_{10}\text{O}_{35}:\text{Mn}^{4+}$," *Optical Materials Express*, vol. 8, no. 9, pp. 2532-2541, 2018, doi: 10.1364/OME.8.002532.
- [16] X. Wang, Y. Wang, J. Yu, Y. Bu, and X. Yan, "Modifying phase, shape and optical thermometry of $\text{NaGdF}_4:2\%\text{Er}^{3+}$ phosphors through Ca^{2+} doping," *Optics Express*, vol. 26, no. 17, pp. 21950-21959, 2018, doi: 10.1364/OE.26.021950.
- [17] W. J. Kim, T. K. Kim, S. H. Kim, S. B. Yoon, H. -H. Jeong, J. -O Song, and T. -Y. Seong, "Improved angular color uniformity and hydrothermal reliability of phosphor-converted white light-emitting diodes by using phosphor sedimentation," *Optics Express*, vol. 26, no. 22, pp. 28634-28640, 2018, doi: 10.1364/OE.26.028634.
- [18] N. C. A. Rashid *et al.*, "Spectrophotometer with enhanced sensitivity for uric acid detection," *Chinese Optics Letters*, vol. 17, no. 8, 2019, doi: 10.3788/COL201917.081701.
- [19] S. Elmalem, R. Giryas, and E. Marom, "Learned phase coded aperture for the benefit of depth of field extension," *Optics Express*, vol. 26, no. 12, pp. 15316-15331, 2018, doi: 10.1364/OE.26.015316.
- [20] N. Anous, T. Ramadan, M. Abdallah, K. Qaraqa, and D. Khalil, "Impact of blue filtering on effective modulation bandwidth and wide-angle operation in white LED-based VLC systems," *OSA Continuum*, vol. 1, no. 3, pp. 910-929, 2018, doi: 10.1364/OSAC.1.000910.
- [21] A. Udupa, X. Yu, L. Edwards, and L. L. Goddard, "Selective area formation of arsenic oxide-rich octahedral microcrystals during photochemical etching of n-type GaAs," *Optical Materials Express*, vol. 8, no. 2, pp. 289-294, 2018, doi: 10.1364/OME.8.000289.
- [22] T. Wei, W. Bo, C. Yan, C. Yeqing, L. Jun, and Z. Qingguang, "Single Pr^{3+} -activated high-color-stability fluoride white-light phosphor for white-light-emitting diodes," *Optical Materials Express*, vol. 9, no. 1, pp. 223-233, 2019, doi: 10.1364/OME.9.000223.
- [23] P. P. Li *et al.*, "Very high external quantum efficiency and wall-plug efficiency 527 nm InGaN green LEDs by MOCVD," *Optics Express*, vol. 26, no. 25, pp. 33108-33115, 2018, doi: 10.1364/OE.26.033108.




- [24] K. Werfli *et al.*, "Experimental Demonstration of High-Speed 4×4 Imaging Multi-CAP MIMO Visible Light Communications," in *Journal of Lightwave Technology*, vol. 36, no. 10, pp. 1944-1951, 2018, doi: 10.1109/JLT.2018.2796503.
- [25] X. Liu *et al.*, "Laser-based white-light source for high-speed underwater wireless optical communication and high-efficiency underwater solid-state lighting," *Optics Express*, vol. 26, no. 15, pp. 19259-19274, 2018, doi: 10.1364/OE.26.019259.
- [26] T. Zhang, X. Zhang, B. Ding, J. Shen, Y. Hu, and H. Gu, "Homo-epitaxial secondary growth of ZnO nanowire arrays for a UV-free warm white light-emitting diode application," *Applied Optics*, vol. 59, no. 8, pp. 2498-2504, 2020, doi: 10.1364/AO.385656.

BIOGRAPHIES OF AUTHORS



Ha Thanh Tung    received the PhD degree in physics from University of Science, Vietnam National University Ho Chi Minh City, Vietnam, he is working as a lecturer at the Faculty of Basic Sciences, Vinh Long University of Technology Education, Vietnam. His research interests focus on developing the patterned substrate with micro- and nano-scale to apply for physical and chemical devices such as solar cells, OLED, photoanode. He can be contacted at email: tunght@vlute.edu.vn.



Huu Phuc Dang    received a Physics Ph.D degree from the University of Science, Ho Chi Minh City, in 2018. Currently, he is a lecturer at the Faculty of Fundamental Science, Industrial University of Ho Chi Minh City, Ho Chi Minh City, Vietnam. His research interests include simulation LEDs material, renewable energy. He can be contacted at email: danghuophuc@iuh.edu.vn.